Effects of Near-Wall Vortices on Wall Shear Stress in a Centrifugal Pump Impeller

SALMAN SHAHID
Department of Mechanical Engineering
Abu Dhabi University
Abu Dhabi, P.O. Box 59911
UNITED ARAB EMIRATES
1062192@students.adu.ac.ae

ABDUL QADER HASAN
Department of Mechanical Engineering
Abu Dhabi University
Abu Dhabi, P.O. Box 59911
UNITED ARAB EMIRATES
1047456@students.adu.ac.ae

SHARUL SHAM DOL
Department of Mechanical Engineering
Abu Dhabi University
Abu Dhabi, P.O. Box 59911
UNITED ARAB EMIRATES
sharulshambin.dol@adu.ac.ae

MOHAMED S. GADALA
Department of Mechanical Engineering
Abu Dhabi University
Abu Dhabi, P.O. Box 59911
UNITED ARAB EMIRATES
mohamed.gadala@adu.ac.ae

MOHD SHIRAZ ARIS
TNB Research Sdn. Bhd.
Kawasan Institusi Penyelidikan
43000 Kajang
Selangor Darul Ehsan
MALAYSIA
shiraz.aris@tnb.com.my

Abstract: - Boundary layer separation and vortex formation cause unappealing deterioration of pump pressure head. The purpose of this research paper is to correlate formation of vortices with near-wall shear stresses resulting in a loss of pump pressure head. This phenomenon is observed at the centrifugal pump impeller tip at various flow rates and impeller rotational velocities through CFD (Computational Fluid Dynamic) analysis. This research paper investigates internal flow in a shrouded centrifugal impeller that is modelled under design flow rate conditions using ANSYS Fluent as its simulation bases solving built-in Navier-Stokes equation, and $k-\omega$ SST turbulence model under steady conditions. Numerical results revealed an increase in wall shear stresses with increasing flow rate ranging from 314.2 Pa to 595.60 Pa at increments that pulsate per flow rate. Flow characteristics, such as evolution of vortices and flow turbulence enhance wall shear stresses increasing the wall skin-friction remarkably leading towards a loss in pressure head. This paper analyzes the vortices and turbulence in flow structures with regards to their influence upon the impeller performance.

Key-Words: - Single-phase; boundary layer separation; pressure gradient; vortex formation; near-wall region; wall shear stress; centrifugal impeller; CFD

Received: January 10, 2021. Revised: February 15, 2021. Accepted: March 3, 2021.
Published: March 5, 2021.

1 Introduction

Electrical Submersible Pumps (ESP) are being utilized at a mass scale as a popular artificial lift mechanism in the oil industry. It consists of a submerged electrical motor powering a multistage centrifugal pump. Having a stable and efficient centrifugal pump is of great importance to the industry [1]. Centrifugal pump is considered an imperative fluid machinery capable of delivering energy to a fluid through rotation of an impeller. This system is implemented in an ESP due to its simple structure and its extensive range of discharge flow rates and heads [2];

However, the flow inside the pump is of complex nature observing the curvature and rotation of the blade. Theoretical as well as experimental studies on internal flow require advance understanding of flow structures and streamwise vortices [3]. Various methods have been utilized to examine internal flow in a centrifugal pump for further study of its flow structures; [3] studied the internal flow through a PIV (Particle image velocimetry) approach in order to investigate the internal fluid flow in a centrifugal pump to

comprehend the discomposure caused on the fluid velocity. Entire focus in a PIV experiment is upon the internal flow occurring in pumps in which flow pattern investigation along with turbulence detection is vital, either in a single phase or dual phase channel at a specific flow rate. Some relevant studies can be found in [4] and [5].

Recent researchers have been solely focused upon two aspects in fluid flow, namely the control of near wall turbulent structures accompanied by wall skin friction [6]. Both these aspects are closely in relation with each other in terms of near wall turbulence structures. A number of researches have been focused on the area of near wall shear stress and near wall flow structures through experimentation. The formation of near wall vortices in internal channels of the pump gives rise to hydraulic loss diminishing the ability of the pump to transfer energy efficiently [7]. Most researchers concluded that wall shear stresses were formed according to near wall streamwise vortices [6]. Presence of emulsion tends to impact the friction factor in flow along with its viscosity and pressure drop [8]

A flow pattern accommodating streamlines developed in concentric circles while the fluid particles are not rotating on their own axis as they are being revolved around a vortex center is known as free or irrotational vortex. These vortices arise through development of a swirling flow that occurs due to its surrounding boundaries as shown in Fig.1 [9]. In applications utilizing an electrical submersible pump, the formation of vortices in between the pump suction side and the suction tank fluid surface calls for air to enter the pump suction which reduces the pumps capacity to provide an increase pressure head [10]. This paper observes fluid vortices as well as vorticity to account for near-wall shear stresses on the walls of the volute and impeller blades in an electrical submersible pump.

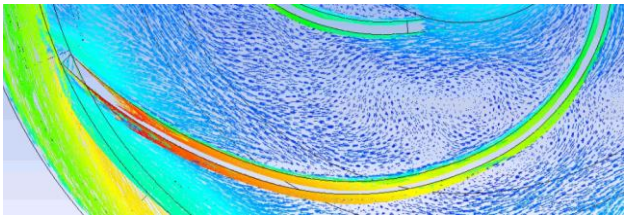

Figure 1: Swirl motion in internal flow at 20 L/min

The formation of vortices in centrifugal pump internal flow at this scale must be avoided. Prior studies have resulted that vortex formation is dependent upon submergence height of the pump, viscosity, velocity at which the fluid exits the pump, density of the fluid in the pump and the geometrical structure of the inlet. There has been tremendous research in observing the vortices; Hurmann von Helmholtz [10] introduced the concepts of vortex dynamics including, vortex line along with derived vorticity equations utilized for incompressible fluid. A uniform inflow leads to development of channel vortices, tip clearance vortices as well as wake vortices. The phenomenon of vortices and vorticity requires in-depth research, since the development of these vortices occurring in the pump can exacerbate the flow structure in the impeller causing massing outpouring of pressure fluctuations and augmentation of cavitation phenomenon. These effects can further lead to instable operation of the pump, including intense vibrations, significant noise and pressure head reductions [9]; therefore, implying that studying the flow of vortices and vorticity in electrical submersible pumps is of utmost importance.

This paper observes the effects of vortices and vorticity in single stage electrical submersible pump to account for the near-wall shear stresses through numerical simulation utilizing ANSYS Fluent and CFD modules. The modelling of GDIWA ISO 9906-Annex A electrical submersible pump provided a comprehensive perspective on the flow profile inside the impeller and the volute for a clear understanding of flow structures and vortices. CFD is utilized for observation of free stream vortices, tip clearance vortices, wake vortices, and wake vortices briefly. Numerical simulation would provide considerably higher flexibility in terms of single-phase parameters including impeller rotational speed as well as intake flow rate. Two-Phase flow in an electrical submersible pump can also be visualized using the same numerical model along with the study of the same parameters. Observation of two-phase flow is crucial to the aviation industry as well where various gaseous fuels are being tested under equivalence ratios [11]

2 Objectives

Objectives that are needed to be met for this research paper includes the following:

1. Observe the variation in vortices along the suction and pressure side of the impeller with varying impeller rotational speed
2. Observe the relationship between the vortices and vorticity patterns with the near-wall shear stresses experienced on the impeller and volute walls
3. Relate the vortices and the vorticity patterns to the losses experienced in centrifugal pumps utilizing streamlines for deduction of various vortices

4. Determine two important aspects of single-phase flow, namely:
   a. Mechanism of vortex formation
   b. Measures to eliminate vortex formation

The above-mentioned objectives are quite heavy in technical details and require understanding of basic incompressible fluid flow structures, but this paper breaks down the concepts for a more understanding perspective on the problem.

3 Simulation Methodology

3.1 Geometrical Model

This research paper utilized a single stage commercial electrical submersible pump designed for mixed flow containing 4 steel blades, a Hub and back shroud. The geometric of the pump was entirely modelled in ANSYS for better recognition in later stages as shown in Fig. 2. The dimensions were measured and kept similar to the physical model of the Electrical Submersible Pump as shown in Fig. 3.

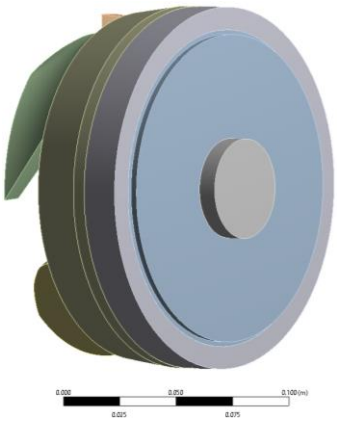

Figure 2: Pump fluid zone utilized for all simulations

Figure 2 illustrates the detailed geometrical model of the ESP considering all indentations, excluding screw and pin holes for sealing the pump preventing leakage during volume fill in. The geometry is modelled incredibly accurately with attention to detail; however, ANSYS is not capable of rendering large amount of minute details; therefore, it is required to fill the exterior geometry forming a fluid zone.

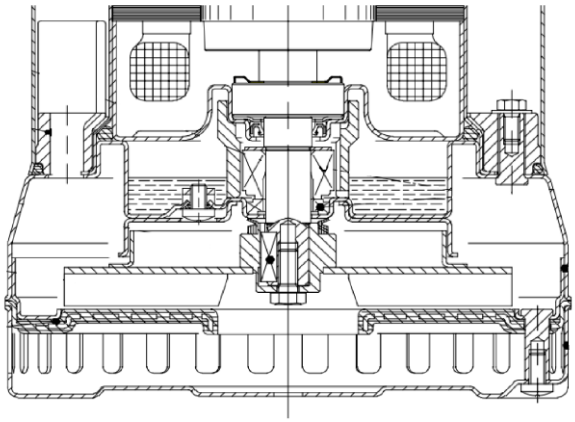

Figure 3: GDIWA Series Electrical Submersible Pump Design

Figure 2 fluid zone is derived from Fig.3 actual pump model through modelling of the casing and filling the model with fluid. All simulations utilized two distinct mesh sizes, a much smaller element size was utilized for the impeller blades and the diffuser due its sophisticated shapes while slightly larger mesh elements occupied the volutes and the inlet. Further details of pump geometry are listed in Table 1 that can be correlated with Fig. 4.

This model provides a complete illustration of the flow from the perspective of the inlet that demonstrates the vorticity of the flow as well as the turbulence all together; however, it does have its limitations in which the model contains a large number of interfaces which increases the computational time and exposes the model to errors.

Table 1: Impeller Parameters

Parameter	Symbol	Value
Inlet diameter (mm)	R_1	42.43
Outlet diameter (mm)	R_2	139.69
Blade inlet height (mm)	H_1	11
Blade outlet height (mm)	H_2	11
No. of blades	n	4
Blade inlet angle (°)	β_1	97.53
Blade outlet angle (°)	β_2	43.74

Figure 4 marks the variables mentioned in Table 1 for a complete understanding of Euler head and various blade angles retrieved from the impeller.

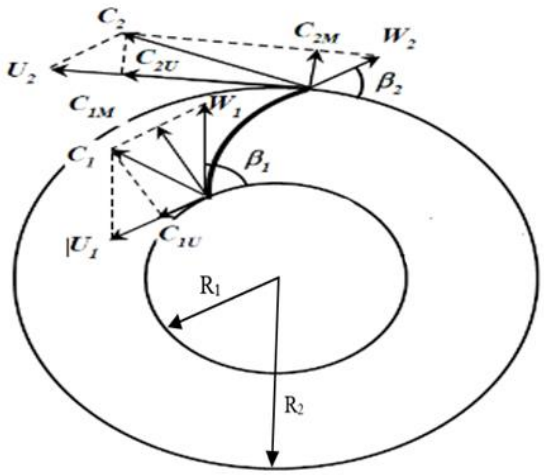

Figure 4: Pump Euler Head and Circumferential angle at the Inlet and Outlet [12]

3.2 Meshing and Grid Division

The complete computing model is derived from the fluid zones of the pump, that includes the impeller, casing, diffuser and inlet pipe. Meshing used for all simulations composed of tetrahedral elements, where priority was given to the impeller and the diffuser through a higher mesh refinement than the volute and inlet. Figure 5 illustrates the mesh generated on the model.

Figure 5: Mesh elements observed on the pump model

Figure 6 provides an illustration on the mesh quality through comparison with manufacturers head on grid discrepancies. Discrepancy between manufacturer head and simulation head decreases with increase in mesh elements from 1.5 to 9 million; however, selecting 7 million elements with just a slight decrease in percentage error in not feasible for this research. 3 million elements provide a good balance between percentage error and computational time.

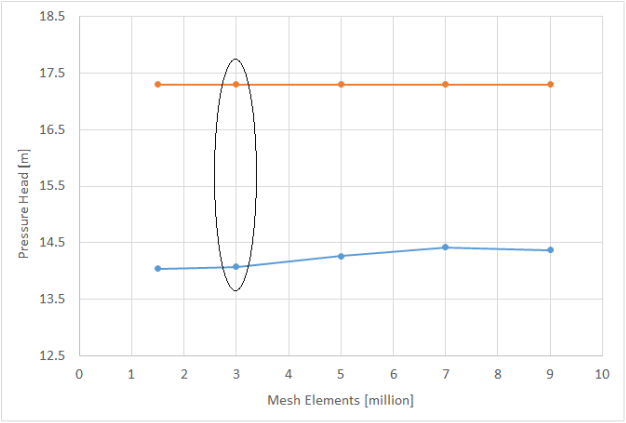

Figure 6: Mesh independency

3.3 Turbulence Model

This centrifugal pump model faced conflict between two of the various turbulence models, namely the K-Omega SST turbulence model and the K-Epsilon RNG turbulence model. Both models are used extensively in the CFD world and are considered to be the most accurate for predictions of flow behavior and flow structures.

CFD solves the Navier-Stokes equation integrated with continuity equation. Since its single phase, a steady state approach is utilized implying that the simulation is independent of time. Equation 1 shows the Steady state Navier-Stokes Equation.

$$\rho(V \cdot \nabla V) = -\nabla p + \mu \nabla^2 V + S \qquad (1)$$

where ρ is the density, V is resultant vector of velocity components, and p is the pressure. The continuity equation is shown in Eq.2.

$$(\nabla \cdot \rho V) = 0 \qquad (2)$$

The main difference between the $k-\omega$ and the $k-\omega$ SST model is the calculation on the turbulent viscosity to note down the transport that happens with the principal turbulent shear stress. This SST model is able to input a cross-diffusion term in the Eq. (1) and (2) that allows better calculation of near-wall shear stresses. The blending function iniates the $k-\omega$ turbulence model in regions near the wall and iniates the $k-\varepsilon$ turbulence model in regions that are away from any surfaces. This allows for much accurate results for a number of flows compared to the standard model [13]. More relevant explanation can be found in [14].

Figure 7 illustrates the similarity between the two models. Variation between $k-\varepsilon$ and $k-\omega$ is significantly closer to each other. These turbulence

models are applied based on the region of the flow study, $k-\varepsilon$ calculates the turbulence away from the wall while $k-\omega$ is closer to the wall; therefore, observing the impact of vortices on near wall shear-stresses requires the use of $k-\omega$ turbulence model.

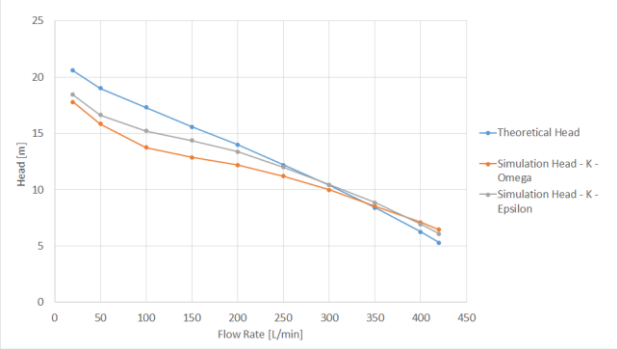

Figure 7: Comparison of $k-\varepsilon$ and $k-\omega$ with manufacturer head

In addition to that, prior researches have also indicated that $k-\omega$ SST model provides an increased accuracy of turbulent flow field calculations. This paper utilizes $k-\omega$ SST turbulence model for simulation due to its ability to solve boundary layer flow near the wall as well as well-developed turbulent flow outside the boundary layer separately [9].

3.4 Boundary Conditions

The impeller rotational speed is set accordingly with the input of flow rate in terms of velocity inlet. Other aspects of pump follow accordingly, such as back shroud, impeller hub and impeller blades. The working fluid in the pump is water. Interfaces are defined according to the model with a total of four interfaces from the inlet to the diffuser outlet.

The main assumption of the model is successful transfer of the entire fluid towards the diffuser and that the results generally converge after a time step of 750 iterations at steady state since the movement of pressure head at the output is at a minimum.

Methods are coupled with entirely being Second order. Report definitions are set to the inlet and the outlet as defined through named selections during the meshing. At steady state, the need for calculating time step size is eliminated and the number of iterations is set to 750 for all cases as during this range of iterations the solution converges.

3.5 Observation

A vortex is defined a mass of certain fluid that objectifies a whirling or a circular motion that proceeds to form a vacuum or cavity at the center of the circle draw the surrounding fluid into this vacuum. Development of vortices within a fluid boundary are less obvious compared to those that account for the vortices located within the solid boundaries. Vortices from a general perspective are illuminated in an unstable flow; furthermore, can lead to new flow arrangements that escalate with rising Reynolds Number [15].

These vortices are laborious to detect through numerical values in a simulation; however, they can be observed through assorted contours and vectors of pressure and velocity. A pressure contour illustrates pressure intensity at different locations in the pump while velocity streamlines or vectors aid in discovering the formation of vortices in the pump as shown in Fig.8 and Fig.9. Fig. 9 illustrates concentric circles and fluid particles that follow rotation on their own axis revolving around a vortex center [10].

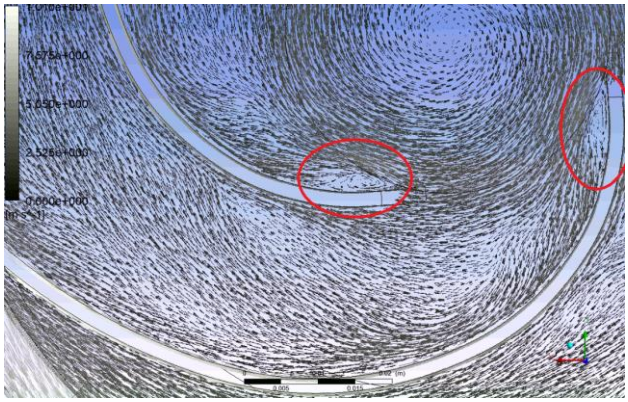

Figure 8: Vortex formation at 100 L/min observed through velocity vectors

Fig.9 illustrates high- and low-pressure zones on the centrifugal pump. The vortex core builds a hydrostatic pressure zone which is the lowest at the vortex core and increases away from the core as emphasized in Fig.8 and 9.

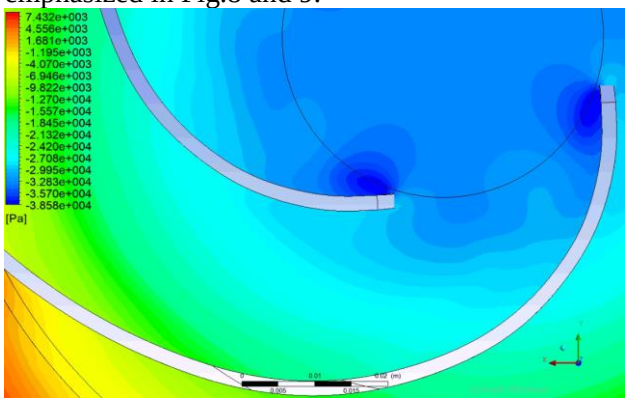

Figure 9: Pressure zones observed through pressure contour

Table 2: Percentage discrepancy between $k-\omega$ SST and Manufactures head at 2850 rpm

Flow Rate [L/min]	Simulation Head [m]	Theoretical Head [m]	% Error
20	17.80	20.6	13.58
50	15.84	19	16.63
100	13.75	17.3	20.51
150	12.87	15.6	17.48
200	12.19	14	12.93
250	11.21	12.2	8.09
300	9.99	10.4	3.91
350	8.54	8.4	1.63
400	7.09	6.25	13.40
420	6.44	5.3	21.51

Using Table 2 the BEP (Best Efficient Point) can be observed to be around 250 to 350 L/min which will be later used for numerical simulation of pump at various RPM for developing the head curve. The BEP is the point where the percentage errors are the least which is at 250 to 350 with 8.09% to 1.63% percentage uncertainty between the simulation head and the manufacturers head. Although, the simulation tends to become highly unstable at higher flow rates of about 400 to 420 L/min due to which the discrepancy between simulation head and manufacturer head increases.

3.7 Simulation Technique

The variation is observed in the flow rates rather than mesh sizing. The flow rates increment according to the manufacturers measured flow rates, going above the mentioned flow rate and set rpm provides for a negative head. Impeller rotational speed is varied from 500, 900, 1500 and 2850 rpm with same measurement techniques and geometry.

The flow rates cannot be maintained at the given impeller rotational speed since a rotation of 500 rpm is not able to withhold the intake flow rate of 420 L/min providing abnormal pressure head values. This issue is tackled by selecting the flow rate prior to the negative head in the pump, this will ensure that at every impeller rotational speed the flow rate is set to the maximum for that specific rotational speed.

This paper is based around the wall shear Equation 3 as the results are discussed based on the wall shear stresses at the impeller tip as well as near-wall shear stresses correlating towards the loss of pressure head in centrifugal pumps [16].

$$\tau = \mu \frac{\partial U}{\partial X} \tag{3}$$

where, μ stands for dynamic viscosity of the fluid, τ is the wall shear stress and $\frac{\partial U}{\partial X}$ is the shear rate of the fluid.

Shear is an important variable in turbulent flow. Study of Kinetic Budget Equation illustrates that a bulk flow regime tends to lose its energy to the turbulence. The energy is utilized to maintain the turbulence in the flow [17].

4 Results and Discussion

Model verification provides an assurance on the maximum error that simulation output values can experience. Figure 10 below provides a comparison between the $k-\omega$ SST simulation output at 2850 rpm and the manufacturers curve at same rpm. This illustrates the reliability of the results retrieved due to verification with the manufacturers pressure head ensuring the results are within the range of percentage error.

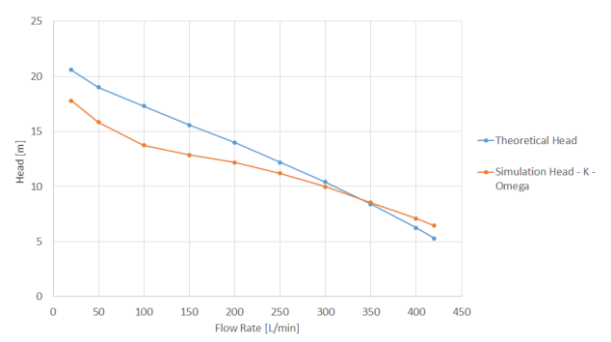

Figure 10: $k-\omega$ SST simulation head comparison with manufacture head

Figure 10 exemplifies the simulation curve matches well with the manufacturer head curve. The average discrepancy for the simulation is within 15% as shown in Table 2 which is acceptable in a numerical simulation and validates the numerical methodology for this paper.

The inlet and outlet pressure that is retrieved from the simulation is then used to calculate the pressure head using Equation 4 and then comparing the pressure head to the manufacturer head.

$$Head = \frac{P_2 - P_1}{9.81 * \rho} \tag{4}$$

where P_2 is the output pressure and P_1 is the inlet pressure.

Figure 11 illustrates the graph comparison between the impeller rotational speed and the flow rates and provides an idea on how the various

pressure heads that are retrieved distinguish between themselves.

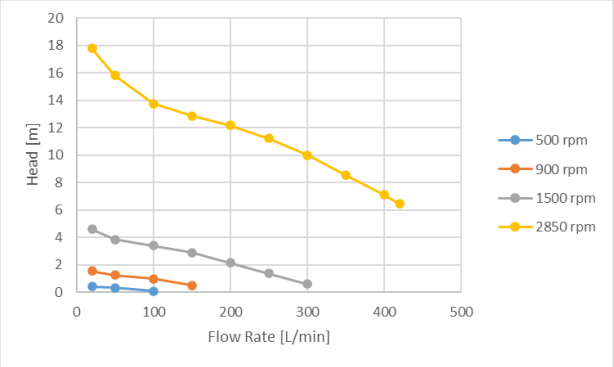

Figure 11: Graph comparison between the rotational speeds and the retrieved pressure head

Figure 12 presents the pressure contour along with the velocity streamlines for 500 rpm at 100 L/min flow rate. The streamlines are able to illustrate the formation of vortices in the flow as well as near the impeller wall.

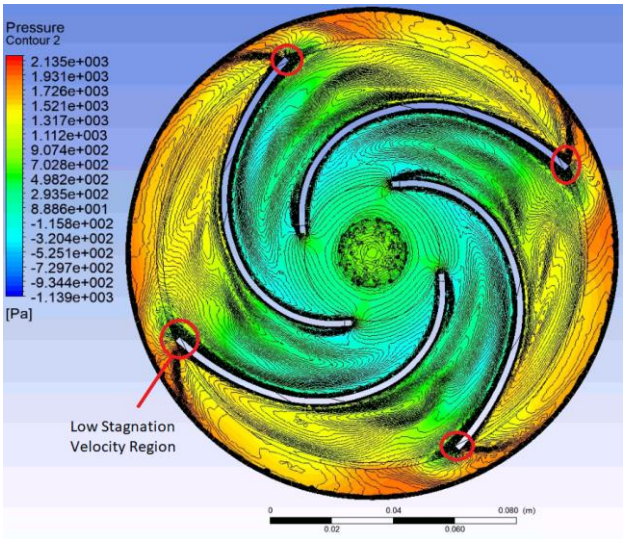

Figure 12: Pressure contour overlap with velocity streamlines

Figure 12 exposes the areas that experience the highest amount of wall shear stresses. The velocity streamlines as shown in Fig. 13 at the impeller blade tips illustrate an area of low stagnation velocity region (marked as red circle in Fig.12) in which the wall shear stresses are at maximum. This solution is based upon Reynolds-averaged Navier-Stokes equations for mean flow field together with a turbulence model [18].

Pressure differences cause bends in streamlines as shown in Fig.14. Suction side of the impellers illustrate a lower pressure compared to the pressure side due to the rotation of the blade. The scale of the vortex at suction side is larger compared to the pressure side along the flow direction; however, it is smaller at the spanwise direction. As the flow decreases the scales of the vortices increases and starts moving towards the inlet and the outlet directions of the pump. Generally, due to the clogging caused by vortices on the suction side, the fluid is accompanied closer together in the pressure side as a result of large Coriolis force experienced [3].

The vortices at the suction and pressure sides are able to increase the absolute tangential velocity and decrease the radial velocity, thereby increasing the head obtained by the flow and reducing the through-flow through the impeller passage. Absolute tangential velocity refers to the linear speed of an object that is moving along a set path. A point fixed on the outer edges of the turntable will move a great distance in one complete rotation than the point at the center.

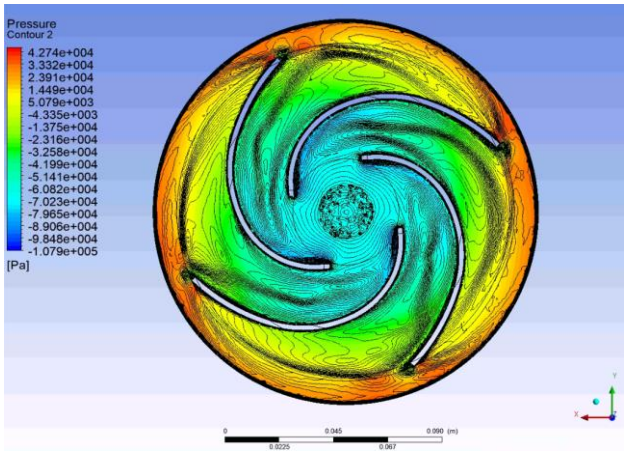

Figure 13: Velocity Streamlines above pressure contour at 2850 rpm and 300 L/min

Figure 13 provides a clear view of streamlines spread across the flow with a similar structure to 500 rpm impeller rotation with high amounts of vorticity closer to the impeller wall. The increase in velocity at the impeller tip indicates flow separation from the surface of the blades. This is due to the instability in vortices caused by shear stresses that allow them to separate from impeller surface and viscously diffuse downstream.

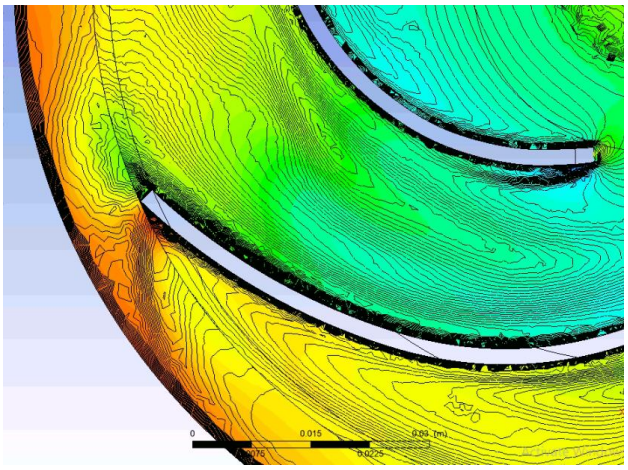

Figure 14: Close up of Velocity Streamlines

Observation of Fig.14 provides an explanation on the vorticial patterns at the impeller tip. Generally, as long as the flow is attached to the surface of the impeller blades, the vortex is being fed by the vorticity from the flow after which it flows downstream freely. The vortex is fed with vorticity until it is capable enough to separate from the surface and flow downstream after which it diffuses downstream for formation of new vortices.

At part-load conditions, a clockwise vortex alongside a counter clockwise vortex appears at both the blade suction and pressure sides. The counterclockwise vortex facilitates the flow movement towards the impeller outlet and the clockwise facilitates opposite. One of them decreases the relative velocity while the other one increases it accordingly [19].

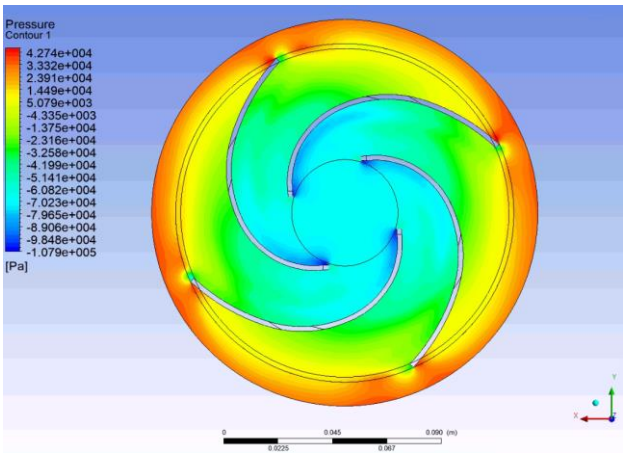

Figure 15: Pressure contour at 2850 rpm

Figure 15 illustrates the pressure variation along the pump at 300 L/min. As the flow rate decreases the flow separation occurs at the suction side of the flow passage; however, as the flow begins to decrease further the flow separation gradually appears in other flow passages, the blade suction and pressure sides. As the flow decreases further, the directional vortices at both sides of the impeller enhance and eventually occupy the entire flow passage with vortices.

Comparison between Fig.15 and Fig.13 illustrate the streamwise vortices are accompanied with sweep and ejection motions. An ejection is basically a low-velocity fluid movement that is directed outward from the wall with the fluid containing negative streamwise fluctuating velocity; whereas, sweep is high speed movement of the fluid that is directed towards the walls with a positive streamwise fluctuating velocity. Both sweep and ejection phenomenon contribute towards the wall shear stresses [20]. The near wall vortical structures present major impact in turbulent transport and are closely related to high skin friction [7]. Figure 13 also provides a demonstration of vortex shedding phenomenon where fluid flow from one side of the blade to other forms a low-pressure zone on the downwind side of the structure which provides it with a fluctuating force acting right angles to the flow direction.

Table 3 illustrates the variation in wall shear stress with respect to the impeller rotational speed. This an increase in the wall shear stresses at the blade tip as the impeller rotational speed increases with respect to the flow rate. This increase is accompanied by the development of vortices at the blade suction and pressure side. Low pressure is correlated with the low-pressure region at the center of a vortex. This low-pressure fluctuates along with vortex formation. The main mechanism related with base pressure is not found in the momentum across certain shear layers, but in the dynamics of the vortices.

Table 3: Wall Shear stresses with relation to flow rates

Flow Rate [L/min]	Wall Shear Stress (Pa)			
	500 rpm	900 rpm	1500 rpm	2850 rpm
20	59.64	218.90	314.20	1052.0
50	70.28	174.20	397.60	1068.0
100	86.87	202.50	428.20	1100.0
150	107.60	222.80	477.90	1169.0
200	-	243.10	501.40	1282.0
250	-	-	517.00	1366.0
300	-	-	545.10	1561.0
350	-	-	595.60	1677.0
400	-	-	-	1500.0
420	-	-	-	1592.0

At impeller rotational speed of 500 rpm, shear stress begins at 59.64 Pa at a flow rate of 20 L/min,

and increases up to 107.60 Pa at a constant increment of 10 to 15 Pa per increase in flow rate. Observing from a relative velocity perspective, as the fluid inlet velocity increases to a value that is a maximum for that impeller rotational speed. The velocity focused upon the suction side of the impeller diminishes while the jet-wake area decreases with respect to the rising flow rate. As the impeller rotates, the flow separation point shift spatially proceeding towards the shifting of secondary flow (Vortex flow) structure followed by change in its intensity [21].

Table 3 also manifests the impact of near-wall vortex formation on the impeller tip as the wall shear stresses begins to ascend gradually for an impeller rotational of 2850 rpm; however, it rises rapidly at 200 L/min and above considered as the Best Efficiency Point of the Pump. Overtime it reaches its peak at 1592 Pa that ought to form large scale vortices in the impeller channels that sheds and grows overtime.

The increase in wall shear stress is a trend that is followed by all the impeller rotational speed from 500 rpm to 2850 rpm at increasing flow rates. This trend is widely related towards the separation of flow at the tips of the impeller. As the inlet flow rate increases periodically, the amount of turbulence formed internally increases, so does the vortices. Turbulence flow induces pressure drag which is comparatively larger than the viscous drag, these enhance due to the boundary layer separation due to an improved momentum transfer by the turbulence flow where the high-pressure gradients drag the fluid towards the wall. Wake size behind an object can be altered through implementation of Flexible Vortex Generators [22]. A flexible cylinder following an oscillating motion will alter the fluid dynamics leading towards stronger turbulence levels [21]. More relevant studies can be found in [23].

As the flow reaches the impeller tip from the pressure side of impeller, near wall vortex formation increases accordingly as per the velocity streamlines in Fig. 16. The boundary layer separation caused at the impeller tips due to the near wall vortices allows for an increase in wall shear stresses at the impeller tip.

Figure 16 manifests a strong evidence about the formation of vortex clusters that are formed due to the phenomenon of boundary layer separation that emerges from the impeller surface assisted by circumferential variation from blade to blade. As time emerges these developed vortex clusters propagate in a radial direction due to the vortex dynamics simulation behavior [24].

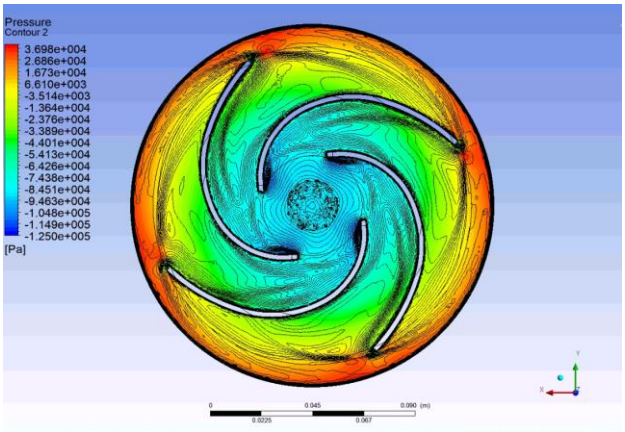

Figure 16: Velocity Streamlines above pressure contour at 2850 rpm and 200 L/min

As the flow rate in the centrifugal pump increases, the separation point detains in regards to the depletion in absolute velocity. Figure 17 presents the graph for variation in wall shear stresses with reference to the flow rates; moreover, observing Fig. 16 allows for an understanding on the continuous generation and shedding of the vortices that are capable of inducing low-frequency pressure pulsations that outcomes a deteriorated performance of the centrifugal pump.

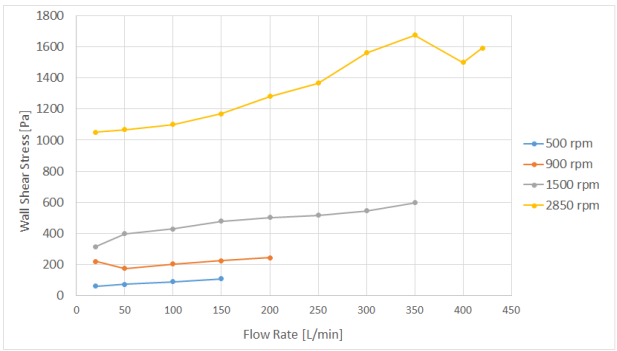

Figure 17: Wall shear stress with respect to Flow rate at various impeller rotational velocity

The vortices that generate at the impeller tip are conventionally unstable attributable to the wall shear stresses that diffuses the vortices viscously downstream generating new vortices in the process. The continuous shedding of the vortices instigates pressure pulsations at the impeller tips as observed in Table 4. These fluctuations in pressure are a result of generation and shedding of the vortices downstream at the impeller tips. The negative sign represents the low pressure point at the impeller tip compared to other regions in the pump.

Table 4: Pressure with regards to impeller rotational speed and flow rates

Flow Rate [L/min]	Pressure at Tip [Pa]			
	500 rpm	900 rpm	1500 rpm	2850 rpm
20	-789.8	8421.0	-7779.0	-20060.0
50	-913.5	7074.0	-4070.0	-14410.0
100	907.4	4829.0	1241.0	-14610.0
150	3686.0	125.2	4425.0	-10000.0
200	-	-4578.0	4407.0	-33890.0
250	-	-	4234.0	-40960.0
300	-	-	6860.0	-41990.0
350	-	-	44400.0	-22030.0
400	-	-	-	-13390.0
420	-	-	-	-10570.0

Observing the vortices with regards to energy, dynamic vortices flowing downstream absorb bulk of the energy from the impeller rotation and this absorption is identical to an additional drag or loss that acts towards the surrounding flow. Overall, it will diminish the efficiency of the centrifugal turbo machinery [25].

5 Conclusion

In conclusion, this research paper investigates the formation of vortices at the centrifugal pump impeller tip and boundary layer separation through numerical simulation. It also provides a breakdown on evolution behavior of the separated vortices as well as the near wall flow in centrifugal pump impeller. The wall shear stress illustrated an increasing trend from 314.20 Pa to 595.60 Pa at 1500 rpm impeller rotational velocity. The formation and shedding of vortices at the impeller tips were illustrated through pulsation in pressure at the impeller tips. The range of impeller rotational velocity from 500 rpm to 2850 rpm provides for a broader perspective on vortex formation and boundary layer separation. This study will allow future impeller designs be compelled to take the distinct flow structures into consideration from the inlet to the diffuser in regards to avoiding flow separation at the impeller tips and pressure head deterioration. Further research in this area must determine how the wall shear stresses are impacted under two-phase flow with gas and liquid being the two phases.

Acknowledgement

We would like to thank Abu Dhabi Award for Research Excellence (AARE) for the research funding.

References

[1] B. Te, A. L. T. Bin and K. Chang-Wei, "Numerical Study of the Single-Phase and Two-Phase Flow in a Centrifugal Pump," *Journal of Applied Mechanics and Materials*, vol. 307, pp. 215 - 218, 13 February 2013.

[2] Y.-J. An and B. R. Shin, "Numerical Investigation of suction vortices behaviour in centrifugal pump," *Journal of Mechanical Science and Technology*, vol. 25, no. 3, pp. 767 - 772, 4 January 2011.

[3] Y. Wang, H. Yang, B. Chen, P. Gao, H. Chen and Z. Zhu, "Analysis of vortices formed in flow passage of a five-bladed centrifugal water pump by means of PIV method," *AIP Advances Mathematical Physics Collection*, 16 July 2019.

[4] M. M. Klazly and G. Bognar, "CFD Study for the Flow Behaviour of Nanofluid Flow over Flat Plate," *International Journal of Mechanics*, vol. 14, pp. 49 - 57, 2020.

[5] Giniatoulline, "Mathematical Modelling of the Rotating Stratified Fluid in a Vicinity of the Bottom of the Ocean," *International Journal of Mechanics*, vol. 13, 2019.

[6] S. Guo and W. Li, "The Effect of Near-Wall Vortices on Wall Shear Stress in Turbulent Boundary Layers," *Scientific Research Journal of Engineering*, pp. 190-196, 21 March 2010.

[7] W. Cao, Z. Jia and Q. Zhang, "Near-Wall Flow Characteristics of a Centrifugal Impeller with Low Specific Speed," vol. 7, no. 8, 5 August 2019.

[8] S. F. Wong and S. S. Dol, "Turbulence Characteristics Study of Emulsified Flow," *WSEAS TRANSACTIONS ON HEAT AND MASS TRANSFER, 14, pp. 45-50, 2019.*

[9] W. Zhang, F. Tang, L. Shi, Q. Hu and Y. Zhou, "Effects of an Inlet Vortex on the Performance of an Axial-Flow Pump," 3 June 2020.

[10] S. Gupta, J. P. Panda and N. Nandi, "A Model Study of Free Vortex Flow," in *International Conference on Theoretical, Applied, Computational and Experimental Mechanics*, Kharagpur.

[11] U. Azimov, E. Tomita, N. Kawahara and S. S. Dol, "Combustion Characteristics of Syngas and Natural Gas in Micro-pilot Ignited Dual-fuel Engine," *International Journal of Mechanical and Mechatronics Engineering*, vol. 6, no. 12, 22 December 2012.

[12] O. Kassem, A. Q. Hasan, S. S. Dol, M. Gadala and S. M. Aris, "CFD Analysis of Electrical Submersible Pumps Handling Single-Phase Flows," *Platform : A Journal of Engineering*, vol. 4, no. 4, 2020.

[13] M. Cable, "An Evaluation of Turbulence Models for the Numerical Study of Forced and Natural Convective Flow in Atria," *International Journal of Automotive and Mechanical Engineering*, vol. 15, no. 2, pp. 5161 - 5177, June 2018.

[14] S. S. Dol, H. B. Chan and S. K. Wee, "FSI Simulation of a Flexible Vortex Generator and the Effects of Vortices to the heat Transfer Process," *Platform: A Journal of Engineering*, vol. 4, no. 2, pp. 58 - 69, 30 June 2020.

[15] H. J. Lugt, "The development of vortices may serve as a paradigm to illustrate how patterns in nature become organized," vol. 73, no. 2, April 1985.

[16] S. S. Dol and S. F. Wong, "Experimental Study on the Effects of Water-in-oil Emulsions to Wall Shear Stress in the Pipeline Flow," *Journal of Applied Fluid Mechanics*, 3 January 2018.

[17] S. S. Dol, K. Perumal, C. H. Bin and W. S. Khur, "Turbulence Characteristics behind a Flexible Vortex Generator," *WSEAS TRANSACTIONS ON FLUID MECHANICS*, 14, pp. 1-7, 2019.

[18] F. Baetke and H. Werner, "Numerical Simulation of Turbulent Flow over surface-mounted obstacles with sharp edges and corners," *Journal of Wind Engineering and Industrial Aerodynamics*, pp. 129 - 147, 5 January 1990.

[19] X. Li, B. Chen, X. Luo and Z. Zhu, "Effects of flow pattern on hydraulic performance and energy conversion characterisation in a centrifugal pump," *International Journal of Renewable Energy*, 11 November 2019.

[20] J. Lelouvetel, F. Bigillon, D. Doppler, I. Vinkovic and J. Y. Champagne, "Experimental investigation of ejections and sweeps involved in particle suspension," 2009 February 12.

[21] R. W. Westra, L. Broersma, K. v. Andel and N. P. Kruyt, "PIV Measurements and CFD Computations of Secondary Flow in a Centrifugal Pump Impeller," *Journal of fluids engineering*, vol. 132, June 2010.

[22] S. S. Dol, H. B. Chan, S. K. Wee and K. Perumal, "The effects of flexible vortex generator on the wake structures for improving turbulence." *IOP Conference Series: Materials Science and Engineering*, vol. 715, no. 1, p. 012070. IOP Publishing, 2020.

[23] S. S. Dol, S. F. Wong, S. K. Wee and J. S. Lim, "Experimental Study on the Effects of Water-in-oil Emulsions to Wall Shear Stress in the Pipeline Flow," *Journal of Applied Fluid Mechanics*, vol. 11, no. 5, 2018.

[24] L. A. Pereira and M. H. HIrata, "Development of the vortex method for centrifugal impeller applications," in *20th International Congress of Mechanical Engineering*, Gramado, 2009.

[25] S. Zhou, P. Lin, W. Zhang and Z. Zhu, "Evolution Characteristics of Separated Vortices and Near-Wall Flow in a Centrifugal Impeller in an Off-Designed Condition," 19 November 2020.